Received 18 December 2015
Revised 20 April 2016
Accepted 19 May 2016

REGULAR ISSUE PAPERS

Natural convection of nanofluids in a cavity: criteria for enhancement of nanofluids

M. Sabour and Mohammad Ghalambaz
Department of Mechanical Engineering, Islamic Azad University of Dezful, Dezful, Iran, and
Ali Chamkha
Department of Mechanical Engineering, Prince Mohammad Bin Fahd University, Al-Khobar, Saudi Arabia and Prince Sultan Endowment for Energy and Environment, Prince Mohammad Bin Fahd University, Al-Khobar, Saudi Arabia

Abstract

Purpose – The purpose of this study is to theoretically analyze the laminar free convection heat transfer of nanofluids in a square cavity. The sidewalls of the cavity are subject to temperature difference, whereas the bottom and top are insulated. Based on the available experimental results in the literature, two new non-dimensional parameters, namely, the thermal conductivity parameter (Nc) and dynamic viscosity parameter (Nv) are introduced. These parameters indicate the augmentation of the thermal conductivity and dynamic viscosity of the nanofluid by dispersing nanoparticles.

Design/methodology/approach – The governing equations are transformed into non-dimensional form using the thermo-physical properties of the base fluid. The obtained governing equations are solved numerically using the finite element method. The results are reported for the general non-dimensional form of the problem as well as case studies in the form of isotherms, streamlines and the graphs of the average Nusselt number. Using the concept of Nc and Nv, some criteria for convective enhancement of nanofluids are proposed. As practical cases, the effect of the size of nanoparticles, the shape of nanoparticles, the type of nanoparticles, the type of base fluids and working temperature on the enhancement of heat transfer are analyzed.

Findings – The results show that the increase of the magnitude of the Rayleigh number increases of the efficiency of using nanofluids. The type of nanoparticles and the type of the base fluid significantly affects the enhancement of using nanofluids. Some practical cases are found, in which utilizing nanoparticles in the base fluid results in deterioration of the heat transfer. The working temperature of the nanofluid is very crucial issue. The increase of the working temperature of the nanofluid decreases the convective heat transfer, which limits the capability of nanofluids in decreasing the size of the thermal systems.

Originality/value – In the present study, a separation line based on two non-dimensional parameters (i.e. Nc and Nv) are introduced. The separation line demonstrates a boundary between augmentation and deterioration of heat transfer by using nanoparticles. Indeed, by utilizing the separation lines, the convective enhancement of using nanofluid with a specified Nc and Nv can be simply estimated.

Keywords Nanofluids, Heat transfer enhancement, Dynamic viscosity number, Laminar natural convection, Thermal conductivity number

Paper type Research paper

The authors acknowledge the financial support of Dezful Branch, Islamic Azad University, Dezful, Iran and Iran Nanotechnology Initiative Council (INIC) for the support of the present study. The authors are grateful to the very competent anonymous reviews for their comment which increased the quality of the present study.

International Journal of Numerical Methods for Heat & Fluid Flow
Vol. 27 No. 7, 2017
pp. 1504-1534

0961-5539
DOI 10.1108/HFF-12-2015-0516

Nomenclature

C = volume fraction of nanoparticles;
Cp = specific heat in constant pressure (J kg^{-1} K^{-1});
g = gravitational acceleration (m s^{-2});
h = thermal convective coefficient (W m^{-2} K^{-1});
k = thermal conductivity coefficient (W m^{-1} K^{-1});
L = length (m);
N = total number of grid nodes;
Nc = thermal conductivity number;
Nu = average Nusselt number;
Nu_x = local Nusselt number;
Nv = thermal viscosity number;
P = pressure (pa);
Pr = Prandtl number;
R = residual of weak form;
Ra = Rayleigh number;
T = temperature (°C);
u = non-dimensional velocity component in x-direction (m s^{-1});
v = non-dimensional velocity component in y-direction (m s^{-1});
x = cartesian coordinate in horizontal direction (m); and
y = cartesian coordinate in vertical direction (m).

Greek symbols

α = thermal diffusivity (m^2 s^{-1});
β = thermal expansion coefficient (K^{-1});
γ = penalty parameter;
θ = non-dimensional temperature;
μ = thermal viscosity (kg s m^{-1});
ρ = density (kg m^{-3}); and
$\xi(x,y)$ = horizontal and vertical coordinate in a unit square.

Subscript

bf = base fluid;
c = cold;
h = hot;
i = residual number;
k = node number;
nf = nanofluid;
p = particles; and
R = ratio.

Superscript

* = Variables in dimensional form.

1. Introduction

In recent years, laminar natural convection heat transfer in enclosures has gained interest of many researchers for application in different practical fields and various industrial sectors (Parvin and Chamkha, 2014; Nasrin *et al.*, 2013; Ismael *et al.*, 2014; Sathiyamoorthy and Chamkha,

2014). In heat removal systems, working based on natural convection heat transfer, there is no need of any external power supply or fan, and, hence, by utilizing these types of systems, the risk of system mechanical failure and the noises and maintains costs would be reduced (Baïri *et al.*, 2014). These advantages have attracted many recent researchers to design heat removal and chemical reactor systems based on the natural convection. The main disadvantage of the natural convection heat transfer is the low rate of heat removal between the fluid and the surface, known as convective heat transfer coefficient, compared to that of the forced convection. Hence, any enhancement in the natural convective heat transfer in enclosures is of great interest. One of the effective ways for achieving a higher convective heat transfer rate is increasing the thermal conductivity of the working fluid. Very recently and by using nano powder technology or chemical methods, a new-engineered type of fluids, nanofluids, has been developed to enhance the thermo-physical properties of the conventional heat transfer fluids. Experiments show that well dispersion of a very low volume fraction of ultra-fine solid particles, nanoparticles, in a conventional heat transfer fluid (base fluid) would significantly increase the thermal conductivity and dynamic viscosity of the mixture (nanofluid) (Ghadimi *et al.*, 2011; Kakaç and Pramuanjaroenkij, 2009; Sundar *et al.*, 2013).Thus, the nanofluids are good potential candidates for natural convective applications due to their enhanced thermal conductivity.

The presence of nanoparticles in a base fluid could alter the thermo-physical properties, such as the thermal conductivity, the dynamic viscosity, the density, the thermal volume expansion and the specific heat capacity of the mixture (Ghadimi *et al.*, 2011; Sundar *et al.*, 2013; Khanafer and Vafai, 2011). The review of thermo-physical properties and convective heat transfer of nanofluids indicates that the presence of a very low volume fraction of nanoparticles in a base fluid would simultaneously enhances the thermal conductivity and dynamic viscosity of the resulting nanofluid (Kakaç and Pramuanjaroenkij, 2009; Khanafer and Vafai, 2011). It is obvious that the increase of the thermal conductivity tends to enhance the heat transfer rate in an enclosure; however, the effect of the augmentation of the dynamic viscosity due to the presence of nanoparticles on the enhancement of the convective heat transfer of nanofluid is not much obvious. Hence, the analysis of the enhancement of convective heat transfer of nanofluids demands further discussions through mathematical modeling or experimental studies. In addition, there are many different factors, such as size, shape, volume fraction and type of nanoparticles, type of the base fluid and working temperature of the system, which could affect the enhancement of the thermal conductivity and the dynamic viscosity of nanofluids. Consequently, any alteration of the thermal conductivity or dynamic viscosity of nanofluids would affect the natural convective heat transfer of the resulting fluid.

There are some very recent studies considering the natural convective heat transfer of nanofluids. Hwang *et al.* (2007) have theoretically examined the natural convective heat transfer of water-Al_2O_3 nanofluids inside a rectangular cavity subject to the temperature difference between top and bottom walls and adiabatic sidewalls. They evaluated the thermal conductivity of the nanofluid using Jang and Choi (2004) model. The dynamic viscosity was evaluated using Einstein (1956) and Pak and Cho (1998) correlations. Jang and Choi (2004) model includes the effect of nanoparticles diameter. The authors (Hwang *et al.*, 2007) found that the increase of the size of nanoparticles leads to deterioration of the rate of the natural convection in the enclosure. Abu-Nada (2009) surveyed improvement of heat transfer in horizontal annuli for water-Al_2O_3 nanofluids. The author reported that the average Nusselt number (i.e. the convective heat transfer rate) could be an increasing or decreasing function of the volume fraction of nanoparticles depending on the magnitude of the Rayleigh number.

Lin and Violi (2010) have investigated the natural convection heat transfer of water-based Al_2O_3 nanofluids inside a quadrilateral enclosure. The outcomes indicate that the decrease of the mean diameter of nanoparticles results in the increase of the heat transfer rate.

The effect of the type of nanoparticles on the convective heat transfer of nanofluids inside a rectangular cavity has been examined by Kahveci (2010). The author performed a comparison for the achieved heat transfer enhancement among different types of spherical nanoparticles including Ag, Cu and Al_2O_3. The result show that the maximum heat transfer enhancement corresponds to Ag nanoparticles. Kahveci (2010) found that the presence of Al_2O_3 nanoparticles could deteriorate the convective heat transfer.

Makinde (2013) studied the effects of viscous dissipation and volume fraction of several nanoparticles over a flat plate. Al_2O_3, TiO_2 and Cu nanoparticles dispersed in the water were studied. The results indicate that increasing the volume fraction of nanoparticles enhances the heat transfer rate. However, intensification of viscous dissipation deteriorates the heat transfer rate. In addition, utilizing Cu nanoparticles produces higher heat transfer rate in comparison with those of TiO_2 and Al_2O_3 nanoparticles. In another study, by considering water as base fluid, the effects of presence of Al_2O_3, TiO_2 and Cu nanoparticles on mixed convection heat transfer about a vertical cone have been surveyed by Patrulescu *et al.* (2014). They found that increasing the volume fraction of nanoparticles can lead to rising of the temperature of nanofluid, thermal conductivity and thermal boundary layer thickness.

Sathiyamoorthy and Chamkha (2014) have investigated the natural convection heat transfer inside a square enclosure. They used a thin partition in different location of the cavity. They considered the boundary conditions similar to Rayleigh–Benard problem in their study. Sathiyamoorthy and Chamkha (2014) found that the rate of heat transfer is reduced when the partition is attached in the bottom wall. In other hand, the presence of partition on the vertical walls can lead to augmentation of heat transfer rate. Baïri *et al.* (2015) provided a correlation between two non-dimensional numbers which are the Rayleigh and Nusselt numbers. They considered the geometry of a closed hemispherical cavity and analyzed the issue for various tilted angles ranging from 0° up to 90°.

Natural convection heat transfer of Cu-water nanofluid inside a C-shaped enclosure has been studied by Mansour *et al.* (2014). They reported that the enhancement of heat transfer rate was evident by increasing the Rayleigh number and the volume fraction of nanoparticles. Noghrehabadi *et al.* (2015) have examined the natural convection heat transfer of CuO-water nanofluids inside a square cavity, whereas two pairs of heat source/sink were mounted on horizontal walls and the vertical walls were insulated. The effects of the presence of thermophresis and Brownian effects on the heat transfer rate were evaluated. The results of the study of Noghrehabadi *et al.* (2015) were in agreement with the results of the study of Mansour *et al.* (2014). Indeed, Noghrehabadi *et al.* (2015) found that increasing the Rayleigh number and the volume fraction of nanoparticles can lead to augmentation of the heat transfer rate.

Free convection heat transfer of water-Cu nanofluid in an enclosure has been investigated by Sheikholeslami *et al.* (2014) in three dimensions. The inner surface of the enclosure was selected as elliptical. Sheikholeslami *et al.* (2014) have defined a heat transfer enhancement ratio parameter in their work and surveyed the effects of thermal conductivity, viscosity and Rayliegh number on heat transfer enhancement.

As seen, most of the available studies in the literature have analyzed the effect of the type and volume fraction of nanoparticles on the convective heat transfer of nanofluids. However, the available experimental data reveal that the size of nanoparticles, the shape of nanoparticles, the type of nanoparticles, the type of the base fluid and the working temperature are also very important (Chandrasekar *et al.*, 2010; Duangthongsuk and Wongwises, 2009; Jeong *et al.*, 2013; Esfe *et al.*, 2014; Agarwal *et al.*, 2013). For example, Jeong *et al.* (2013) examined the effect of different shapes of nanoparticles on the thermal conductivity and dynamic viscosity of nanofluids. They used water as the base fluid and prepared two types of nanofluid samples, containing the rectangular and spherical ZnO nanoparticles. The researchers measured the

thermal conductivity and dynamic viscosity of the samples and found that the samples containing the rectangular nanoparticles show higher thermal conductivity and dynamic viscosity compared to those containing spherical nanoparticles. Agarwal *et al.* (2013) considered the effect of the size of nanoparticles on the thermal conductivity and dynamic viscosity of nanofluids. They utilized kerosene as the base fluid to synthesize samples of the kerosene-Al_2O_3 nanofluids. The authors prepared two types of samples by dispersing different volume fractions of 21 and 40 nm spherical alumina nanoparticles in the kerosene. The measurement of the thermal conductivity and dynamic viscosity of the samples reveals that the thermal conductivity and dynamic viscosity of the nanofluid enhances as the size of nanoparticles reduces. Duangthongsuk and Wongwises (2009) synthesized water-TiO_2 nanofluid with 21 nm nanoparticles. They examined the effect of the working temperature on the dynamic viscosity and thermal conductivity of nanofluid. The authors conducted measurements for three working temperatures of 15°C, 25°C and 35°C. The results indicate that the increase of the working temperature raises the thermal conductivity and declines the dynamic viscosity of the water base TiO_2 nanofluid.

Most common methods of synthesis of nanofluids are divided into single-step and two-step methods. In the single-step method, the nanoparticles are synthesized and dispersed in a base fluid without any intermediate steps. In contrast, in the two-step method, first nanoparticles are needed to be produced and then they will be dispersed in the base fluid. The two mentioned methods have advantages and disadvantages. In the single-step method, nanoparticles with a smaller size can be dispersed in a base fluid. In this method, the size of nanoparticles is more uniform and the sedimentation issues are limited. On the other hand, commercial production of a nanofluid as well as the production of a nanofluid containing high volume fraction of nanoparticles by using the single-step method is difficult and expensive. The pulsed wire evaporation and vacuum evaporation onto a running oil substrate are sub-categories of the single-step method (Lee *et al.*, 2012; Agarwal *et al.*, 2013).

The commercial production of nanofluids using the two-step method is convenient, but the most important defect of this method is the aggregation and settlement of nanoparticles. To resolve this problem, the nanoparticles with a specified volume fraction will be dispersed inside a base fluid via stirring, ultrasonication and high-pressure techniques. In addition, surfactants of nanoparticles, change in pH and ultrasonic vibration methods have a key role in enhancement of nanofluid stability (Chandrasekar *et al.*, 2010; Esfe *et al.*, 2014; Agarwal *et al.*, 2013; Duangthongsuk and Wongwises, 2009; Jeong *et al.*, 2013).

Nanofluids are mainly a well dispersed and stable solution of nanoparticles which could be remained stable for days (Ghadimi and Metselaar, 2013; Lotfizadeh Dehkordi *et al.*, 2013; Sadollah *et al.*, 2013). For example, Ghadimi and Metselaar (2013) have prepared samples of TiO_2 nanoparticles (25 nm) dispersed in water using different techniques of ultrasonication. In addition, the stability of water-TiO_2 nanofluid was provided by adding a surfactant. The results show that most of samples are almost stable for seven days when the nanofluid is quiescent. In the convective heat transfer applications, in which the nanofluid is in motion, longer stability time could be expected.

Jeong *et al.* (2013) used an aqueous solution (two-step method) to synthesize nanofluids containing ZnO nanoparticles with the volume fraction ranging from 0.05 per cent upto 5 per cent. Jeong *et al.* (2013) dispersed ZnO nanoparticles in 25°C water base fluid by the stirring technique. Two types of nanoparticles shapes, rectangular and spherical shape nanoparticles, were also studied. Furthermore, the dynamic light scattering technique was utilized to determine the size of nanoparticles. The ultrasonic vibration method was applied to create more stability of suspended nanoparticles. By using the zeta potential criteria, the stability level of

rectangular and spherical ZnO nanoparticles in water base fluid was evaluated. The results reveal that the synthesized water-ZnO nanofluid shows a suitable stability.

Agarwal *et al.* (2013) applied a two-step method to production of kerosene-Al_2O_3 nanofluid. Ultrasonication, surfactant of nanoparticles and change in pH methods were performed for synthesizing a stable kerosene-Al_2O_3 nanofluid. The size of nanoparticles was measured by Malvern–Zetasizer technique. Agarwal *et al.* (2013) have interestingly observed a change in color of kerosene-Al_2O_3 nanofluid from white to gray in the ultrasonication process.

Chandrasekar *et al.* (2010) utilized the two-step method to synthesize a water-Al_2O_3 nanofluid. Al_2O_3 nanoparticles were suspended in water base fluid through the ultrasonication technique. They applied the ultrasonic vibration method on sample for about 6 h until reaching a stable solution. These researchers, Chandrasekar *et al.* (2010), did not use any booster methods of nanofluid stability such as change in pH and surfactant additives.

Duangthongsuk and Wongwises (2009) synthesized a water-TiO_2 nanofluid by using the stirring technique. They also applied the ultrasonic vibration method to enhance the stability of nanofluid. They have measured the pH level of the solution for several volume fractions of nanoparticles. The results indicate that the synthesized nanofluid shows a neutral pH and subsequently a good stability.

Esfe *et al.* (2014) dispersed MgO nanoparticles in water base fluid by utilizing the ultrasonication technique. They applied a surfactant method to enhance the stability of the synthesized nanofluid. They measured the pH of the synthesized nanofluid and found that difference between nanofluid pH and iso-electric point of MgO nanoparticles is high. Hence, water-MgO nanofluid was properly stable. In Table I, the dispersing techniques and stability methods for synthesizing stable nanofluids are summarized.

In a benchmark study, Buongiorno *et al.* (2009) have analyzed the thermal conductivity of eight different synthesized samples of nanofluids in 30 distinct laboratories around the world. The outcomes demonstrate that the thermal conductivity of nanofluids is a linear function of the volume fraction of nanoparticles. In a parallel study with Buongiorno *et al.* (2009), Venerus *et al.* (2010) in a benchmark study have examined the dynamic viscosity of different synthesized samples of nanofluids in different laboratories and using different measurement techniques. The results indicate that the dynamic viscosity of nanofluids is also a linear function of the volume fraction of nanoparticles. Although the thermal conductivity and dynamic viscosity of nanofluids are a linear function of the volume fractions of nanoparticles, the slope of these observed linear functions highly depends on the different aspects of nanofluids such as the size of nanoparticles, shape of nanoparticles, the type of nanoparticles, the type of the base fluid, the synthesized method and the working temperature (Ghadimi *et al.*, 2011; Kakaç and Pramuanjaroenkij, 2009; Sundar *et al.*, 2013; Khanafer and Vafai, 2011; Buongiorno *et al.*, 2009; Venerus *et al.*, 2010).

Table I. Dispersing techniques and stability methods of synthesized nanofluids

References	Dispersing technique	Stability method	Made nanofluid
Ghadimi and Metselaar (2013)	Ultrasonication	Surfactant	water-TiO_2
Jeong *et al.* (2013)	Stirring	Ultrasonic vibration	water-ZnO
Agarwal *et al.* (2013)	Ultrasonication	Surfactant and change in PH	kerosene-Al_2O_3
Chandrasekar *et al.* (2010)	Ultrasonication	Ultrasonic vibration	water-Al_2O_3
Duangthongsuk and Wongwises (2009)	Stirring	Ultrasonic vibration	water-TiO2
Esfe *et al.* (2014)	Ultrasonication	Surfactant	water-MgO

In the present study, based on the results of Buongiorno *et al.* (2009) and Venerus *et al.* (2010) and following the study of Zaraki *et al.* (2015), we have simply formulated the thermal conductivity and dynamic viscosity of nanofluid as a liner function of volume fraction of nanoparticles using definition of *Nc* and *Nv*. However, different aspects of nanofluids, including shape, size and type of nanoparticles, temperature effects and method of preparation, could be seen in *Nc* and *Nv*. Then, we have reported separation lines, indicating the margin for enhancement of using nanofluids, as a function of *Nc* and *Nv*. The graphs indicating the separation lines could be seen as a convenient way to conclude about potential natural convective enhancement of a synthesized nanofluid.

As mentioned, Hwang *et al.* (2007), Abu-Nada (2009), Lin and Violi (2010) and Kahveci (2010) have conducted case studies to analyze the convective heat transfer of nanofluids in enclosures. In each research, only very few aspects of nanofluids was analyzed; in addition, the utilized models for thermal conductivity and dynamic viscosity were also different. For example, Hwang *et al.* (2007) and Abu-Nada (2009) have theoretically studied the effect of the type and volume fraction of nanoparticles; Lin and Violi (2010) have analyzed the effect of the size of the nanoparticles; Kahveci (2010) studied the effect of type of nanoparticles on the natural convective heat transfer of nanofluids in enclosures. The results of these studies show that the presence of nanoparticles in a base fluid could enhance or deteriorate the natural convective heat transfer, which depends on the induced enhancement in the thermal conductivity and dynamic viscosity of the synthesized nanofluid. Hence, reaching a general conclusion about the enhancement of nanofluids and discussing about the enhancement of new possible synthesized nanofluids demands a comprehensive general approach.

Now, assume that a researcher has synthesized a new type of nanofluid and has measured its thermal conductivity and dynamic viscosity for different volume fractions of the nanoparticles. The measurements show enhancements in both of the thermal conductivity and dynamic viscosity. At this stage, the researcher or a customer needs to know: Does this new nanofluid enhance the convective heat transfer? The following questions are also arising: How does the volume fraction of nanoparticles affect the convective heat transfer? How does the Rayleigh number affect the convective heat transfer of the nanofluid compared to the base fluid?

In our previous research (Zaraki *et al.*, 2015), we have tried to tackle this problem by analyzing the effect of different aspects of nanofluids such as the effect of size of nanoparticles, shape of nanoparticles and type of nanoparticles on the natural convective heat transfer of nanofluids for external flows using the boundary layer theory. The results indicate that the type of the nanoparticles and the type of the base fluid are the most important parameters, which affect the heat transfer enhancement of nanofluids. The deterioration of heat transfer was also observed for some cases. However, it is worth mentioning that the natural convection in the boundary layer for external flows is fundamentally different from the natural convective heat transfer in enclosures. In the external flows, the pressure gradients are negligible and the effect of flow circulation could be also neglected, but, in an enclosure, the flow circulates in the system and the pressure gradients are significant.

In the present work, a general non-dimensional study has been conducted to analyze the effect of the presence of nanoparticles on the natural convective heat transfer of nanofluids in an enclosure. Two new non-dimensional parameters, namely, thermal conductivity parameter and dynamic viscosity parameter, are introduced and utilized in the general analysis of nanofluids. The introduced non-dimensional parameters could be a function of the affective parameters of nanofluid such as size of nanoparticles, shape of nanoparticles, type of nanoparticles, type of the base fluid and the working temperature. Using the introduced non-dimensional parameters, some criteria for analysis of the enhancement of nanofluids is

presented for the first time. Ultimately, using the proposed non-dimensional parameters, various aspects of nanofluids such as the effect of size, shape and type of nanoparticles, the type of the base fluid and the working temperature on the natural convective heat transfer of nanofluids in enclosures have been theoretically analyzed as case studies. To the best of the author's knowledge, the results of the present study are new and have not been published before.

2. Mathematical model

Consider the steady state laminar natural convection of a nanofluid in a square cavity (enclosure) of the size L with adiabatic top and bottom walls and isothermal vertical walls. Figure 1 illustrate a schematic representation of the geometry of model, coordinate system and the boundary conditions. Following the pioneer works of Kahveci (2010) and Hussain and Hussein (2014), the governing equations for the conservation of the mass, momentum and energy are written as:

$$\frac{\partial u^*}{\partial x^*} + \frac{\partial v^*}{\partial y^*} = 0 \tag{1}$$

$$\rho_{nf}\left(u^*\frac{\partial u^*}{\partial x^*} + v^*\frac{\partial u^*}{\partial y^*}\right) = -\frac{\partial \mathrm{p}^*}{\partial x^*} + \mu_{nf}\left(\frac{\partial^2 u^*}{\partial x^{*2}} + \frac{\partial^2 u^*}{\partial y^{*2}}\right) \tag{2}$$

$$\rho_{nf}\left(u^*\frac{\partial v^*}{\partial x^*} + v^*\frac{\partial v^*}{\partial y^*}\right) = -\frac{\partial \mathrm{p}^*}{\partial y^*} + \mu_{nf}\left(\frac{\partial^2 v^*}{\partial x^{*2}} + \frac{\partial^2 v^*}{\partial y^{*2}}\right) + \rho_{nf} g\beta(T - T_c) \tag{3}$$

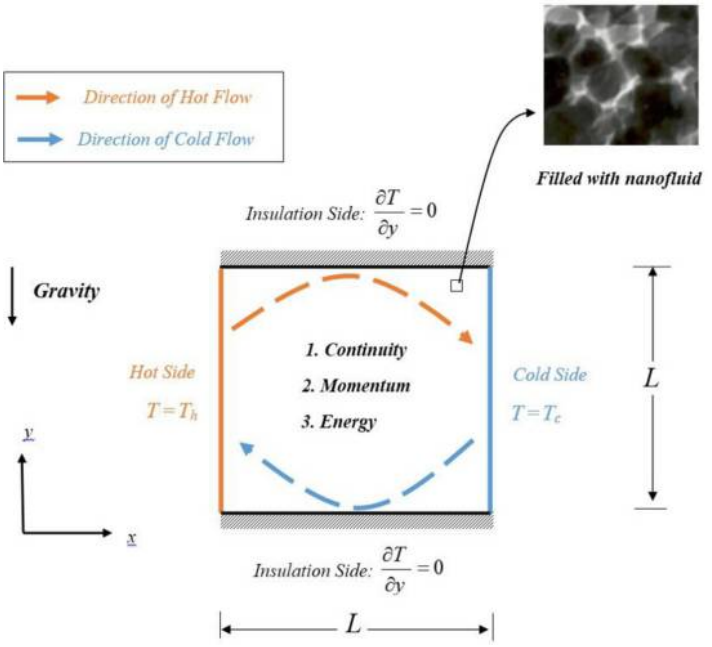

Figure 1.
Schematic diagram of physical model

$$u^* \frac{\partial T}{\partial x^*} + v^* \frac{\partial T}{\partial y^*} = \frac{k_{nf}}{\rho_{nf} Cp_{nf}} \left(\frac{\partial^2 T}{\partial x^{*2}} + \frac{\partial^2 T}{\partial y^{*2}} \right) \tag{4}$$

where p^*, and T are the pressure and temperature of the nanofluid, respectively. The quantities of ρ_{nf}, μ_{nf}, Cp_{nf} and k_{nf} are density, dynamic viscosity, specific heat capacity and thermal conductivity coefficient of the nanofluid, respectively. According to problem definition in Figure 1, the corresponding boundary conditions for equations (1)-(4) are:

$$u^*(-L/2, y^*) = v^*(-L/2, y^*) = 0,\ u^*(L/2, y^*) = v^*(L/2, y^*) = 0,$$
$$T(-L/2, y^*) = T_h,\ T(L/2, y^*) = T_c \tag{5}$$

$$u^*(x^*, 0) = v^*(x^*, 0) = 0\,,\ u^*(x^*, L) = v^*(x^*, L) = 0\,,\ \left.\frac{\partial T}{\partial y^*}\right|_{(x^*,0)} = 0\,,\ \left.\frac{\partial T}{\partial y^*}\right|_{(x^*,L)} = 0 \tag{6}$$

Using the following non-dimensional parameters:

$$x = \frac{x^*}{L},\ y = \frac{y^*}{L},\ u = \frac{u^* . L}{\alpha_{bf}},\ v = \frac{v^* . L}{\alpha_{bf}},\ \theta = \frac{T - T_c}{T_h - T_c},\ p = \frac{L^2 . p^*}{\rho_{bf} . \alpha_{bf}^2} \tag{7}$$

The non-dimensional equations for continuity, momentum and energy equations are obtained as:

$$\frac{\partial u}{\partial x} + \frac{\partial v}{\partial y} = 0 \tag{8}$$

$$u \frac{\partial u}{\partial x} + v \frac{\partial u}{\partial y} = -\frac{\rho_{bf}}{\rho_{nf}} \frac{\partial p}{\partial x} + \frac{\mu_{nf}}{\mu_{bf}} \frac{\rho_{bf}}{\rho_{nf}} \mathrm{Pr} \left(\frac{\partial^2 u}{\partial x^2} + \frac{\partial^2 u}{\partial y^2} \right) \tag{9}$$

$$u \frac{\partial v}{\partial x} + v \frac{\partial v}{\partial y} = -\frac{\rho_{bf}}{\rho_{nf}} \frac{\partial p}{\partial y} + \frac{\mu_{nf}}{\mu_{bf}} \frac{\rho_{bf}}{\rho_{nf}} \mathrm{Pr} \left(\frac{\partial^2 v}{\partial x^2} + \frac{\partial^2 v}{\partial y^2} \right) + \mathrm{RaPr}\theta \frac{(\rho\beta)_{nf}}{\rho_{nf}\beta_{bf}} \tag{10}$$

where $Ra = (\rho g \beta_{bf} \Delta T L^3)/(\alpha_{bf} \nu_{bf})$ and $Pr = \nu_{bf}/\alpha_{bf}$ and $\alpha_{bf} = k_{bf}/\rho_{bf} Cp_{bf}$:

$$u \frac{\partial \theta}{\partial x} + v \frac{\partial \theta}{\partial y} = \frac{k_{nf} (\rho \mathrm{cp})_{nf}}{k_{bf} (\rho \mathrm{cp})_{bf}} \left(\frac{\partial^2 \theta}{\partial x^2} + \frac{\partial^2 \theta}{\partial y^2} \right) \tag{11}$$

The boundary conditions are also transformed into the following non-dimensional form:

$$u(-0.5, y) = v(-0.5, y) = 0,\ u(+0.5, y) = v(+0.5, y) = 0,$$
$$\theta(-0.5, y) = 1,\ \theta(+0.5, y) = 0 \tag{12}$$

$$u(x, 0) = v(x, 0) = 0,\ u(x, 1) = v(x, 1) = 0,\ \left.\frac{\partial \theta}{\partial y}\right|_{(x,0)} = 0 \left.\frac{\partial \theta}{\partial y}\right|_{(x,1)} = 0 \tag{13}$$

The density, heat capacity and the volumetric thermal expansion coefficient for the nanofluid can be evaluated using the following relations (Khanafer and Vafai, 2011):

$$\rho_{nf} = (1 - C)\rho_{bf} + C\rho_p \tag{14}$$

$$(\rho C_p)_{nf} = (1 - C)(\rho C_p)_{bf} + C(\rho C_p)_p \tag{15}$$

$$(\rho\beta)_{nf} = (1 - C)(\rho\beta)_{bf} + C(\rho\beta)_p \tag{16}$$

The benchmark studies reported by Buongiorno *et al.* (2009) and Venerus *et al.* (2010) indicate that the thermal conductivity and dynamic viscosity for nanofluids are linear functions of volume fraction of nanoparticles as:

$$\frac{k_{nf}}{k_{bf}} = 1 + NcC \tag{17}$$

$$\frac{\mu_{nf}}{\mu_{bf}} = 1 + N\nu C \tag{18}$$

where Nc and Nv are introduced in our previous research (Zaraki *et al.*, 2015) as thermal conductivity parameter and dynamic viscosity parameters, respectively. These parameters could be depended on various aspects of nanofluids including the size, type and shape of nanoparticles and also the working temperature and the type of the base fluid. Table IV indicates values of Nc and Nv which are obtained through experimental studies available in literature.

Here, the parameter of interest for convective heat transfer in the cavity are the local Nusselt number ($Nu_x = hx/k$) and the average Nusselt number (Nu). The local Nusselt number of nanofluid is defined as:

$$Nu_x = -\left(\frac{k_{nf}}{k_{bf}}\right)\left(\frac{\partial\theta}{\partial x}\right)_{x=0} \tag{19}$$

and the average Nusselt Number of nanofluid as:

$$Nu = -\left(\frac{k_{nf}}{k_{bf}}\right)\int_{y=0}^{y=1}\left(\frac{\partial\theta}{\partial x}\right)_{x=0} dy \tag{20}$$

In the above equations, the thermal conductivity ratio can be evaluated using equation (17), which results in the following equations for the local and average Nusselt numbers:

$$Nu_x = -(1 + NcC)\left(\frac{\partial\theta}{\partial x}\right)_{x=0} \tag{21}$$

$$Nu = -(1 + NcC)\int_{y=0}^{y=1}\left(\frac{\partial\theta}{\partial x}\right)_{x=0} dy \tag{22}$$

Now, let us assume that the cavity is solely filled with a nanofluid as a uniform homogeneous fluid. In this case, the Rayleigh number and the Prandtl number can be introduced as:

$$Ra_{nf} = \frac{\rho_{nf}^2 C_p \beta_{nf} \Delta T L^3}{k_{nf} \mu_{nf}} \text{ and } Pr_{nf} = \frac{C_p \mu_{nf}}{k_{nf}} \tag{23}$$

where the dynamic viscosity and thermal conductivity can be substituted from equations (17) and (18) which results in:

$$Ra_{nf} = \frac{\rho_{nf}^2 C_p \beta_{nf} \Delta T L^3}{k_{bf} \mu_{bf} (1 + NcC)(1 + NvC)} \text{ and } Pr_{nf} = \frac{(C_p)_{nf} \mu_{bf}}{k_{bf}} \frac{(1 + NvC)}{1 + NcC} \tag{24}$$

As will be discussed later, the variations of density, thermal capacity and thermal expansion coefficient for nanofluids are low, and, hence, Rayleigh and Prandtl number for a nanofluid can be approximated as:

$$Ra_{nf} \approx \frac{Ra_{bf}}{(1 + NcC)(1 + NvC)} \text{ and } Pr_{nf} \approx Pr_{bf} \frac{1 + NvC}{1 + NcC} \tag{25}$$

Using equation (25), many thermo-physical behaviors of natural convection of nanofluids could be explained, which will be discussed later. In the text, the Rayleigh number for the base fluid will be simply called Rayleigh number and will be indicated by (Ra); the Rayleigh number for the nanofluid will be also indicated by Ra_{nf}.

3. Numerical method and validation

The system of partial differential equations, equations (8)-(11), along with the boundary conditions, equations (12) and (13), were transformed to weak form and solved numerically utilizing Galerkin finite element method (Basak *et al.*, 2006a, 2006b; Reddy, 1993). The continuity equation, equation (8), is used as a constraint to satisfy the mass conservation. Hence, the constraint for continuity equation is introduced as a penalty parameter (γ) in the momentum equations as described by Reddy (1993). Therefore, the pressure is written as:

$$P = -\gamma \left(\frac{\partial u}{\partial x} + \frac{\partial v}{\partial y} \right) \tag{26}$$

Using equation (26), the momentum equations are reduced as:

$$u \frac{\partial u}{\partial x} + \nu \frac{\partial u}{\partial y} = \frac{\rho_{bf}}{\rho_{nf}} \gamma \frac{\partial}{\partial x} \left(\frac{\partial u}{\partial x} + \frac{\partial v}{\partial y} \right) + \text{Pr} \left(\frac{\partial^2 u}{\partial x^2} + \frac{\partial^2 u}{\partial y^2} \right) \tag{27}$$

$$u \frac{\partial v}{\partial x} + v \frac{\partial v}{\partial y} = \frac{\rho_{bf}}{\rho_{nf}} \gamma \frac{\partial}{\partial y} \left(\frac{\partial u}{\partial x} + \frac{\partial v}{\partial y} \right) + Pr \left(\frac{\partial^2 v}{\partial x^2} + \frac{\partial^2 v}{\partial y^2} \right) + \frac{(\rho \beta)_{nf}}{\rho_{nf} \beta_{bf}} (\text{RaPr} \theta) \tag{28}$$

Thus, in the above equations, the continuity equation (8) is satisfied for very large values of the penalty parameter ($\gamma = 10^7$) (Reddy, 1993). Now, the velocities (u and v), as well as the temperature, are expanded invoking a basis set $\{\xi_k\}_{k=1}^N$ as:

$$u \approx \sum_{k=1}^{N} u_k \xi_k(x,y), \quad v \approx \sum_{k=1}^{N} v_k \xi_k(x,y), \quad \theta \approx \sum_{k=1}^{N} \theta_k \xi_k(x,y). \tag{29}$$

for $-0.5 < x < +0.5$ and $0 < y < 1$. It should be noted that the basis functions for u and v velocities and the temperature are the same, and, thus, the total number of nodes variables is N. Invoking the Galerkin finite element method, the nonlinear residual for the governing equations of momentum [equations (27) and (28)], and the energy [equation (11)], at nodes of internal domain Ω is derived as:

$$R_i^1 = \sum_{k=1}^{N} u_k \int_\Omega \left[\left(\sum_{k=1}^{N} u_k \xi_k \right) \frac{\partial \xi_k}{\partial x} + \left(\sum_{k=1}^{N} v_k \xi_k \right) \frac{\partial \xi_k}{\partial y} \right] \xi_i dxdy + \gamma \frac{\rho_{bf}}{\rho_{nf}} \sum_{k=1}^{N} u_k \int_\Omega \frac{\partial \xi_i}{\partial x} \frac{\partial \xi_k}{\partial x} dxdy + \gamma \frac{\rho_{bf}}{\rho_{nf}} \sum_{k=1}^{N} v_k \int_\Omega \frac{\partial \xi_i}{\partial x} \frac{\partial \xi_k}{\partial y} dxdy + \mathrm{Pr} \sum_{k=1}^{N} u_k \int_\Omega \left[\frac{\partial \xi_i}{\partial x} \frac{\partial \xi_k}{\partial x} + \frac{\partial \xi_i}{\partial y} \frac{\partial \xi_k}{\partial y} \right] dxdy \quad (30)$$

$$R_i^2 = \sum_{k=1}^{N} v_k \int_\Omega \left[\left(\sum_{k=1}^{N} u_k \xi_k \right) \frac{\partial \xi_k}{\partial x} + \left(\sum_{k=1}^{N} v_k \xi_k \right) \frac{\partial \xi_k}{\partial y} \right] \xi_i dxdy + \gamma \frac{\rho_{bf}}{\rho_{nf}} \sum_{k=1}^{N} u_k \int_\Omega \frac{\partial \xi_i}{\partial y} \frac{\partial \xi_k}{\partial x} dxdy + \gamma \frac{\rho_{bf}}{\rho_{nf}} \sum_{k=1}^{N} v_k \int_\Omega \frac{\partial \xi_i}{\partial y} \frac{\partial \xi_k}{\partial y} dxdy + \mathrm{Pr} \sum_{k=1}^{N} v_k \int_\Omega \left[\frac{\partial \xi_i}{\partial x} \frac{\partial \xi_k}{\partial x} + \frac{\partial \xi_i}{\partial y} \frac{\partial \xi_k}{\partial y} \right] dxdy + Ra\mathrm{Pr} \int_\Omega \left(\sum_{k=1}^{N} \theta_k \xi_k \right) \xi_i dxdy \quad (31)$$

$$R_i^3 = \sum_{k=1}^{N} \theta_k \int_\Omega \left[\left(\sum_{k=1}^{N} u_k \xi_k \right) \frac{\partial \xi_k}{\partial x} + \left(\sum_{k=1}^{N} v_k \xi_k \right) \frac{\partial \xi_k}{\partial y} \right] \xi_i dxdy + \sum_{k=1}^{N} \theta_k \int_\Omega \left[\frac{\partial \xi_i}{\partial x} \frac{\partial \xi_k}{\partial x} + \frac{\partial \xi_i}{\partial y} \frac{\partial \xi_k}{\partial y} \right] dxdy \quad (32)$$

where for the basis function the Bi-quadratic functions with three point Gaussian quadrature are adopted to evaluate the integrals in the above equations. In the momentum equations, the terms incorporating the penalty parameter (γ) are computed using the two point Gaussian quadrature using the reduced integration penalty formulation (Reddy, 1993). The nonlinear residual equations, equations (30)-(32), are solved by Newton–Raphson method to compute the coefficients of the expansions (i.e. u_k, v_k and θ_k) in equation (29). The detailed solution procedure could be found in Basak *et al.* (2006a, 2006b). Additionally, the computational domain comprises grid points in which the discretized equations were implemented. A non-uniform grid was adopted in both x and y directions. The grid was clustered in the vicinity of the walls with the ration of 1.05. The iteration process commenced until the residuals for the momentum residual equation, i.e. $j = 1$ and 2, and the heat equation, i.e. $j = 3$, satisfy $\sqrt{\Sigma (R_i^j)^2} \leq 10^{-7}$.

The solution procedure, in the form of an in-house computational fluid dynamics code, has been validated successfully against the work conducted by Kahveci (2010) and Turan

et al. (2011). Kahveci (2010) has examined the natural convection heat transfer of water-AL_2O_3 nanoparticles in a square cavity. Kahveci (2010) utilized the Maxwell (1881) model for evaluation of the thermal conductivity of nanofluids. The Brinkman (1952) model was also utilized to evaluate the dynamic viscosity of nanofluids. Using curve-fitting on the Maxwell (1881) and Brinkman (1952) models for thermal conductivity and dynamic viscosity, it is found that $Nc = 3.3$ and $Nv = 2.88$ are appropriate values for evaluating the thermal conductivity and dynamic viscosity of water-AL_2O_3.

Figure 2(a) compares the evaluated values of the average Nusselt number (Nu) obtained in the present study when $Nc = 3.3$ and $Nv = 2.88$ and the results reported by Kahveci (2010) for different values of Rayleigh numbers ($Ra = 10^4$, 10^5 and 10^6). In addition, the average Nusselt number is also evaluated and plotted in Figure 2(a). As seen, there is a very good agreement between the results of the present study and those reported by Kahveci (2010). Figure 2(b) compares the temperature profiles in a cavity evaluated using the present numerical method and those reported by Turan *et al.* (2011) when $C = 0$. This figure also shows a good agreement between the results of present study and the results available in literature.

The agreement with the previous studies supports the capability of the assumed linear relations, expressed in equations (17) and (18), for dealing with the convective heat transfer analysis of nanofluids. It should be noted that the introduction of the thermal conductivity parameter (Nc) and the dynamic viscosity parameter (Nv) would significantly facilitate the general analysis of nanofluids in the convective heat transfer problems. It should be also noticed that the curves of Nusselt number, velocity or temperatures for arbitrary combinations of the parameters of Nv and Nc represents different behavior of synthesized nanofluids regardless of the synthesized method, shape, size, type of nanoparticles or other affective parameters. Ultimately, as the dynamic viscosity and thermal conductivity behavior of a synthesized nanofluid can be expressed by a specified set of $\overline{Nv}$ and Nc parameters, the convective heat transfer of the nanofluid can be easily concluded from the evaluated plots. Therefore, in the section of results, the effect of variation of these parameters, i.e. Nc and Nv, on the convective heat transfer of nanofluids (average Nusselt number) will be analyzed as a general analysis of nanofluids.

4. Grid check

To check the grid independency of the solution, the calculations were repeated for several grid sizes. The average Nusselt number for three grid sizes of 50×50, 100×100 and 200×200 are obtained for various volume fractions of nanoparticles. The results are summarized in Table II. As seen, the grid size of 100×100 could provide acceptable accuracy for calculations within the range of engineering applications, and, hence, the results of the paper are obtained for this size of grid.

5. Result and discussion

This section is divided into two parts. In the first part, the non-dimensional analysis of convective heat transfer of nanofluids regarding to thermal conductivity and dynamic viscosity parameters is discussed. In the second section, various aspects of nanofluids including the effect of size shape and type of nanofluids for convective heat transfer of nanofluids is analyzed.

5.1 Non-dimensional analysis

Analysis of the introduced non-dimensional parameters, i.e. Nc and Nv, for different synthesized nanofluid shows that these values could practically vary in the range of 3 to 20.

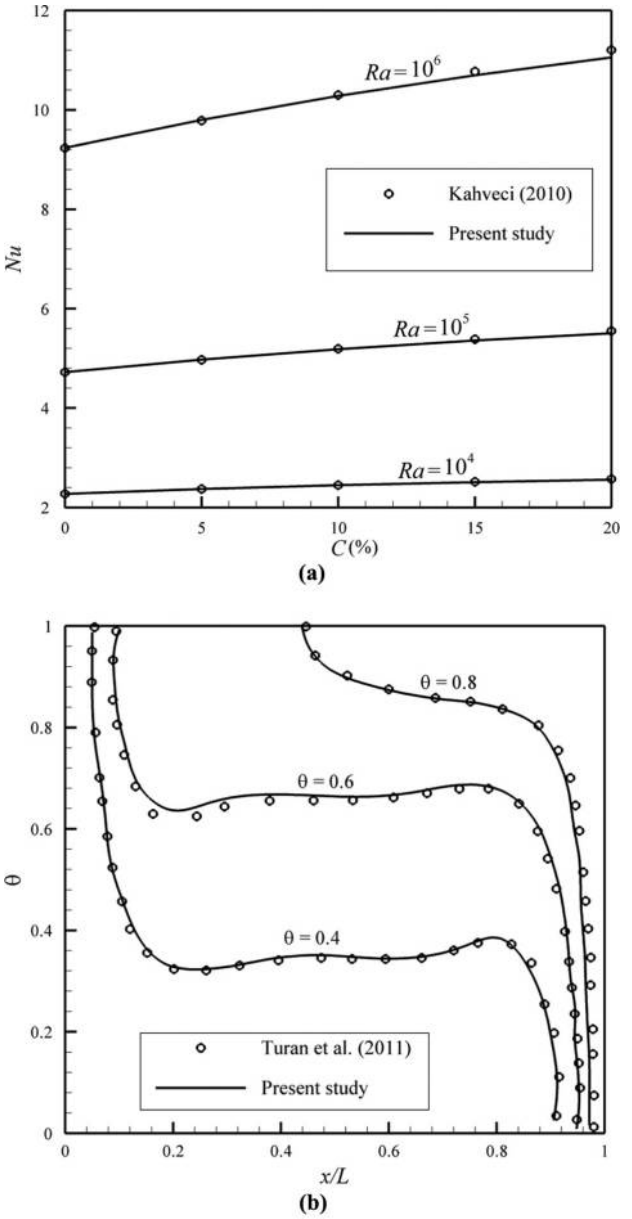

Notes: (a) Nusselt number as a function of the volume fraction of nanoparticle for various value of Rayleigh Numbers; (b) contour of non-dimensional temperature of the base fluid (i.e. $C = 0$ per cent) when $Ra = 10^5$ and $Pr = 1{,}000$ (for right to left heat transfer)

Figure 2.
Comparison of the results with the literature

The ratios of ρ_{nf}/ρ_{bf} and $(\rho c)_{nf}/(\rho c)_{bf}$ are also practically about unity for nanofluids. For example, these ratios for 2 per cent volume fractions of zinc oxide (ZnO) nanoparticles in water are 1.094 and 0.9943, respectively, and for 2 per cent volume fractions of alumina (AL_2O_3) nanoparticles in kerosene are 1.08 and 1.018, respectively. Therefore, the values ρ_{nf}/ρ_{bf} and $(\rho c)_{nf}/(\rho c)_{bf}$ are assumed equal to one for convenience.

The effect of the variation of Prandtl number on the average Nusselt number was plotted and analyzed, but the figure has not been depicted here for the sake of brevity. The outcomes show that the increases of the Prandtl number from very small values ($Pr = 0.01$) to the values about $Pr = 7.0$ significantly increases the average Nusselt number. However, the further increase of the Prandtl number shows very smooth and insignificant effects on the average Nusselt number. As the Prandtl number for the most of nanofluids and base fluids is about $Pr = 7.0$ and higher the effect of the variation of the Prandtl number on the average Nusselt number (convective heat transfer) can be neglected.

Figure 3 shows the ratio of the average convective heat transfer coefficient of the nanofluid (h_{nf}) to the average convective heat transfer coefficient of the base fluid (h_{bf}),

Table II.
The calculated average Nusselt number for different grid sizes for AL_2O_3-based nanofluid for various concentration of alumina nanoparticles in water when $Ra = 10^5$

C (%)	Grid size (50 × 50)	Grid size (100 × 100)	Grid size (200 × 200)
0	4.72551	4.72215	4.72125
5	4.97844	4.97532	4.97449
10	5.18582	5.18294	5.18218

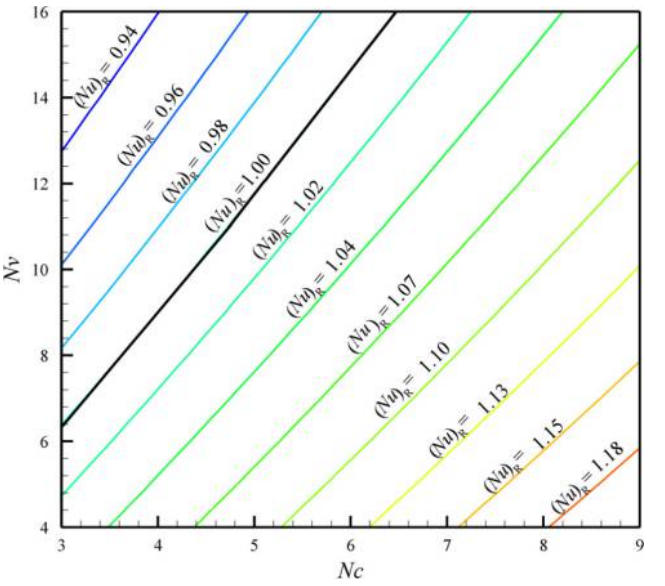

Figure 3.
Contours of average Nusselt number ratio $[(Nu)_R = h_{nf}/h_{bf}]$ for $Ra = 10^5$, in $Pr = 7$ and $C = 5$ per cent (for nanofluids)

i.e. h_{nf}/h_{bf}, as a function of thermal conductivity (*Nc*) and dynamic viscosity (*Nv*) parameters when $C = 5$ per cent, $Pr = 7.0$ and $Ra = 10^5$. It is clear that when $h_{nf}/h_{bf} > 1$, the presence of nanoparticles in the base fluid results in the enhancement of the convective heat transfer. In contrast, when $h_{nf}/h_{bf} < 1$, the presence of nanoparticles in the base fluid could deteriorate the convective heat transfer. Figure 3 shows that the increase of *Nc* increases the convective heat transfer; however, the raise of *Nv* declines the convective heat transfer. In Figure 3, the bold-black curve shows the curve of $h_{nf}/h_{bf} = 1$. This curve demonstrates a boundary between the areas, in which utilizing nanofluid could enhance or deteriorate the convective heat transfer. Here, we call this line as the separation-line. Equation (25) indicates that the increase of both *Nc* and *Nv* tends to decrease the magnitude of the Rayleigh number for a nanofluid. The variation of *Nc* and *Nv* also affects the Prandtl number. The analysis of the effect of variation of the Prandtl number of the convective heat transfer indicates that the variation of the Prandtl number on the heat transfer is important when the Prandtl number is very small (lower than 6). As the Prandtl number for nanofluids is commonly about 7 or higher, the variation of the Prandtl number does not induce significant effect on the strength of natural convection in the cavity. It is clear that the decrease of the Rayleigh number (by the presence of nanoparticles) would decrease the strength of the convection heat transfer in the cavity. However, it should be noted that the increase of *Nc* induces a direct effect on the heat transfer which is obvious in equation (22). The enhancement of *Nc* tends to directly enhance the heat removal from the wall by the enhancement in thermal conductivity of the base fluid. Therefore, it is clear that the increase of *Nv* tends to monotonically decrease the heat transfer in the cavity, but the increase of *Nc* induces two opposite effects. As mentioned, the increase of *Nc* tends to enhance the heat transfer by the increase of heat removal from the wall, but it also tends to reduce the heat transfer by weakling the natural convective heat transfer in the cavity. Therefore, situations in which the presence of nanoparticles reduce or enhance the heat transfer in the cavity could be sought. However, it should be noted that the presence of nanoparticles in the base fluid simultaneously affects the Rayleigh number and the thermal conductivity of the resulting nanofluid. The variation of the Rayleigh number of the nanofluid would nonlinearly affect the convective heat transfer in the cavity. Hence, discussion about the overall enhancement of nanofluids needs more attention, especially due to the nonlinear behavior of the fluid with the variation of the Rayleigh number. As a conclusion, we have plotted the separation lines to more contently discuss the enhancement behavior of homogeneous nanofluids.

The conventional models of Maxwell (1881) and Brinkman (1952) for thermal conductivity and dynamic viscosity propose the values of *Nc* and *Nv* about 3. Considering these values, i.e. $Nc \approx Nv \approx 3.0$, and attention to Figure 3 shows that utilizing nanofluids results in enhancement of heat transfer in the cavity. This observation is in good agreement with the results of case studies reported by Kahveci (2010) and Turan *et al.* (2011). However, some of nanofluids do not follow the Maxwell (1881) and Brinkman (1952) models, and, hence, the presence of nanoparticles may induce values of *Nc* and *Nv*, in which the corresponding nanofluid be placed somewhere above the separation-line and results in deterioration of the convective heat transfer in the cavity. This possibility will be discussed later in the section of case studies.

Figure 4 illustrates separation lines (i.e. $h_{nf}/h_{bf} = 1.0$) as a function of *Nv* and *Nc* for several Rayleigh numbers ranging from 10^4 up to 10^8. Indeed, when the Rayleigh number is small, the dominant heat transfer mechanism is the conduction of the nanofluid. As indicated in equation (25), any augmentation of the dynamic viscosity because of the presence of nanoparticles monotonically tends to reduce the convective heat transfer in cavity. When the Rayleigh number (Ra_{bf}) is low, the fluctuations of the Rayleigh number

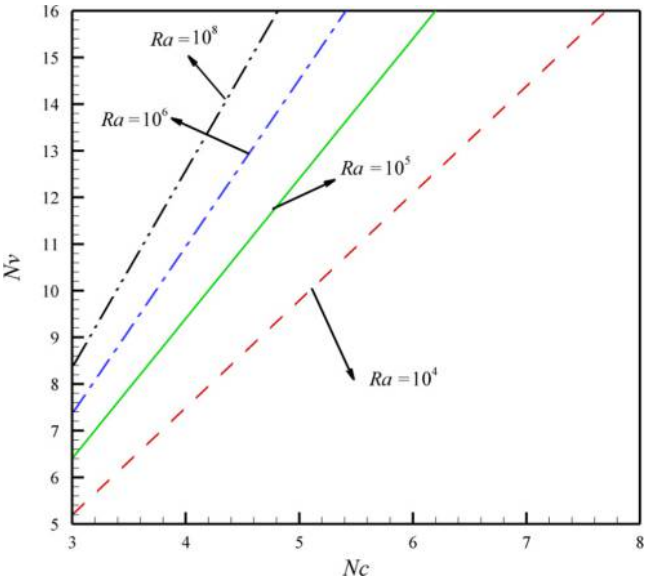

Figure 4.
Effects of Rayleigh number on separation line ($h_{nf}/h_{bf} = 1$) in $C = 5$ per cent

could strongly affect the pattern of the convective heat transfer in the cavity and consequently the convective heat transfer. Therefore, the variation of Nv which directly can influence Rayleigh number of the nanofluid [through equation (25)] is important. When Rayleigh number (Ra_{bf}) is high, its fluctuations does not significantly affect the patterns of convective heat transfer in the cavity. Hence, as seen, as the Rayleigh number increases, the inclination of separation lines also increases. This figure in agreement with Figure 3 shows that when the Rayleigh number is high the dominant parameter for heat transfer enhancement is the thermal conductivity parameter (Nc) which directly affect the heat transfer in the cavity by enhancing the conductive heat removal from the wall. Indeed, by considering a fixed enhancement in thermal conductivity (i.e. fixed value of Nc) and increasing the Rayleigh number, the corresponding separation value of the dynamic viscosity parameter (Nv) also increases. This effect indicates that a nanofluid which may be not of practical interest for enhancement of the heat transfer in a low Rayleigh number (Ra_{bf}) could be of practical enhancement for a high value of Rayleigh number.

As the alteration of Rayleigh number alters the separation lines, it is also possible that the presence of the nanoparticles results in the enhancement of the convective heat transfer for high Rayleigh numbers but deterioration of the convective heat transfer for low values of Rayleigh number. Thus, utilizing a nanofluid for a specific size of cavity and a prescribed temperature difference (a fixed Rayleigh number for the base fluid) may results in the enhancement of heat transfer but for another temperature difference or cavity size (another Rayleigh number) may results in deterioration of the heat transfer.

Figure 5 shows the average Nusselt number of the nanofluid as a function of the volume fraction of nanoparticles for various values of the thermal conductivity and dynamic viscosity parameters when $Ra = 10^5$. This figure reveals that the increase of the volume fraction of nanoparticles boosts the possible enhancement or possible deterioration of heat transfer.

For example, consider a nanofluid with $Nc = 3$ and $Nv = 6$. This set of parameters, i.e. the nanofluid with $Nc = 3$ and $Nv = 6$, indicates a point in Figure 4. For the case of $Ra = 10^5$, this

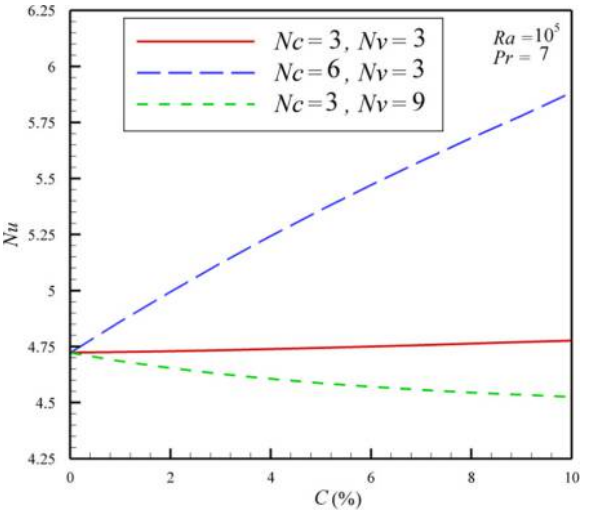

Figure 5.
The average Nusselt number as a function of the concentration of nanoparticles for various values of *Nc* and *Nv*

point is below the separation line, and, hence, the enhancement of heat transfer is expected due to the presence of nanoparticles. For this case, it is clear that the increase of the volume fraction of nanoparticles (*C*) tends to boost the observed enhancement. In contrast, the pair of $Nc = 3$ and $Nv = 9$ indicates a point in Figure 4 which placed above the separation line of $Ra = 10^5$, and, hence, the presence of nanoparticles results in the deterioration of the heat transfer. As seen in Figure 5, the increase of the nanoparticles volume fraction tends to boost this effect and, hence, results in more deterioration of the heat transfer.

Figure 6 shows the effect of Rayleigh number on the average Nusselt number for various values of nanoparticles concentrations when $Pr = 7.0$ and the thermal conductivity parameter (*Nc*) and the dynamic viscosity parameter (*Nv*) are within the comparable magnitude, i.e. $Nc = Nv = 3.0$. As seen in this case, the presence of nanoparticles enhances the natural convective heat transfer. When the Rayleigh number is small, the effect of the presence of nanoparticles on the average Nusselt number is negligible. As the Rayleigh number increases, the effect of the presence of nanoparticles intensifies.

5.2 Case studies

In this section, the effect of the size of nanoparticles, the shape of nanoparticles, the type of nanoparticles, the type of the base fluid and the working temperature on the convective heat transfer of nanofluids is analyzed. Two types conventional fluids, water and kerosene, are chosen as the base fluids. The thermo-physical properties of these fluids are shown in Table III. Three temperatures of 15°C, 25°C and 35°C were considered to analysis the effect of the working temperature on the convective heat transfer of nanofluids. Four types of nanoparticles, Al_2O_3, TiO_2, ZnO, MgO, are selected to examine the effect of the type of nanoparticles. The thermo-physical properties of the nanoparticles are depicted in Table IV. Two shapes of nanoparticles, rectangular and spherical, are also considered to examine the effect of the shape of nanoparticles on the convective heat transfer. In summary, nine samples of nanofluids from five references are adopted in the present study. These samples and the corresponding values of *Nc* and *Nv* are depicted in Table V.

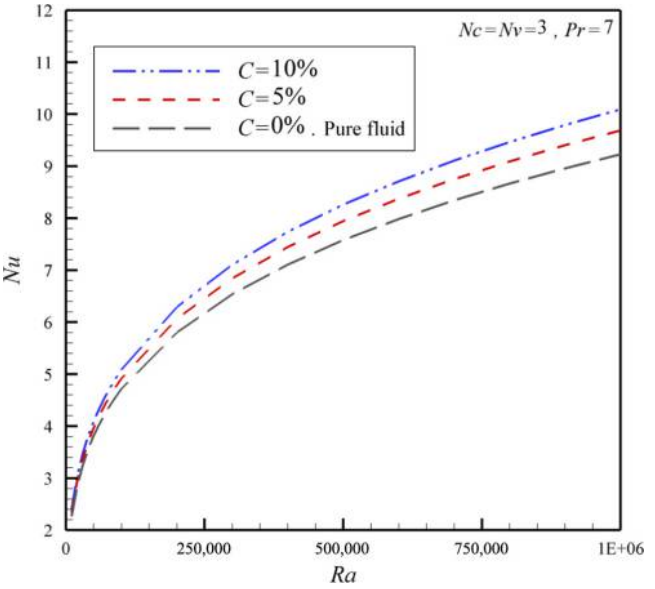

Figure 6.
Effect of volume fraction of nanoparticles on Nusselt number in several Rayleigh number

Type	T(°C)	ρ(kg m^{-3})	Cp(J kg^{-1} K^{-1})	β(K^{-1}) $\times 10^{-4}$	k(W m^{-1} K^{-1})	α(m^2 s^{-1}) $\times 10^{-7}$	Pr
Water	15	999.10	4,185.5	1.188	0.588	1.406	8.117
Water	25	997.05	4,181.4	2.253	0.606	1.454	6.161
Water	35	994.04	4,178.4	3.222	0.622	1.499	4.837
Kerosene	25	790.00	2,010.0	10.000	0.101	0.631	28.10

Source: Toolbox (2013a, 2013b)

Table III.
Thermo-physical properties of water and kerosene

Type	ρ(kg m^{-3})	K(W m^{-1}K^{-1})	Cp(J kg^{-1}K^{-1})	α(m^{2}s^{-1}) $\times 10^{-5}$	β(K^{-1}) $\times 10^{-6}$
Al_2O_3	3950	40	773	1.310	17.4
TiO_2	4250	8.4	692	0.286	12.2
ZnO	5700	25	523	0.581	8.7
MgO	3580	30	879	0.953	33.6

Source: Sarkar (2011) and Ceramaret (2013)

Table IV.
Thermo-physical properties of nanoparticles

The thermal conductivity parameter (Nc) and dynamic viscosity parameter (Nv) for the samples are evaluated using linear curve-fitting for equations (17) and (18) on the reported experimental measurements in the literature. It should be noted that there are scarce experimental works, in which both of the dynamic viscosity and thermal conductivity of the nanofluid have been measured and reported simultaneously. Hence, a very careful attention in literature review was made for selecting these nine samples.

Case	References	T (°C)	Type	Base fluid	Size (nm)	Shape	Nc	Nv
C1	Duangthongsuk and Wongwises (2009)	15	TiO_2	Water	21	Spherical	4.25	4.47
C2	Duangthongsuk and Wongwises (2009)	25	TiO_2	Water	21	Spherical	3.87	7.65
C3	Duangthongsuk and Wongwises (2009)	35	TiO_2	Water	21	Spherical	3.42	9.57
C4	Jeong *et al.* (2013)	25	ZnO	Water	150	Rectangular	3.86	13.3
C5	Jeong *et al.* (2013)	25	ZnO	Water	40	Spherical	3.26	10.88
C6	Esfe *et al.* (2014)	25	MgO	Water	40	Spherical	7.70	12.05
C7	Chandrasekar *et al.* (2010)	25	Al_2O_3	Water	43	Spherical	3.37	16.68
C8	Agarwal *et al.* (2013)	25	Al_2O_3	Kerosene	21	Spherical	20.1	20.23
C9	Agarwal *et al.* (2013)	25	Al_2O_3	Kerosene	44	Spherical	14.1	15.62

Source: Zaraki *et al.* (2015)

Table V.
The evaluated value of *Nc* and *Nv* for different samples of nanofluids

The samples of C1-C9, which were summarized in Table V, can be divided into five categories as follows:

(1) the effect of the type of base fluids (Group No. 1);

(2) effect of the size of nanoparticles (Group No. 2);

(3) the effect of the shape of nanoparticles (Group No. 3);

(4) the effect of the type of nanoparticles (Group No. 4); and

(5) effect of the working temperature (Group No. 5).

The details of these categories are summarized in Table VI.

Table V shows the evaluated values of the average Nusselt number for the different samples of nanofluids. To obtain the results of this table, the physical properties of Tables II and III were utilized to evaluate the values of the Prandtl number, the density ratio (ρ_{nf}/ρ_{bf}) as well as buoyancy ratios $(\rho\beta)_{nf}/(\rho_{nf}\beta_{bf})$. The results for Group No. 1 in Table VI reveal that kerosene-AL_2O_3 nanofluid (Agarwal *et al.*, 2013), containing about 44 nm spherical nanoparticles, show higher Nusselt number than that of the water-Al_2O_3 nanofluid (Chandrasekar *et al.*, 2010). Based on the values of *Nc* and *Nv* in Table V, the kerosene-Al_2O_3 and water-Al_2O_3 nanofluids are taken place below and above the separation line of $Ra = 10^5$,

No.	*T*(°C)	Nanoparticles type	Base fluid	Size *(nm)*	Shape	Nusselt no.	Case
1	25	AL_2O_3	Water	43	Spherical	4.308	C7
	25	AL_2O_3	Kerosene	44	Spherical	5.710	C9
2	25	AL_2O_3	Kerosene	44	Spherical	5.710	C9
	25	AL_2O_3	Kerosene	21	Spherical	6.134	C8
3	25	ZnO	Water	40	Spherical	4.514	C5
	25	ZnO	Water	150	Rectangular	4.488	C4
4	25	ZnO	Water	40	Spherical	4.514	C5
	25	MgO	Water	40	Spherical	5.059	C6
5	15	TiO_2	Water	21	Spherical	5.055	C1
	25		Water	21	Spherical	4.755	C2
	35		Water	21	Spherical	4.590	C3

Table VI.
Comparison of results of average Nusselt number between pair cases in $C = 5\%$ and $Ra = 10^5$

respectively. Hence, the presence of nanoparticles enhances the natural convective heat transfer for kerosene-Al_2O_3 but deteriorates the natural convective heat transfer for water-Al_2O_3.

Here, Figure 7 is plotted to depict the effect of Rayleigh number and volume fraction of nanoparticles on the average Nusselt number for the nanofluids in Group No. 1. This figure, in agreement with the results of Table VI, shows higher values of Nusselt number for Kerosene-Al_2O_3. In Figure 7, the gray line of $C = 0$ per cent shows the average Nusselt number for the base fluids (water and kerosene). Table III indicates that the Prandtl numbers for water and kerosene are high (about 7.0 and higher); hence, as mentioned in non-dimensional analysis section, the variation of the Prandtl does not show any significant effect on the average Nusselt number. Thus, the gray continues line, i.e. $C = 0$ per cent, in Figure 7, represents the average Nusselt number for both water and kerosene base fluids. Figure 7 also clearly shows that the presence of alumina (Al_2O_3) nanoparticles in the water (C7) deteriorates the heat transfer, but the presence of the same nanoparticles in the kerosene (C9) significantly enhances the average Nusselt number. The same trend of results was also observed in the boundary layer analysis of natural convection heat transfer of nanofluids in the study of Zaraki *et al.* (2015). The discussion about the results of Table VI will be followed in Figures 8-13 in more details.

Figure 8(a) and 8(b) show the isotherm contours for the water-Al_2O_3 and kerosene-Al_2O_3 nanofluids. In these figures, the isotherms of the nanofluid and the base fluid are compared. As seen, the presence of nanoparticles smoothly changes the patterns of the isotherms. Figure 9(a) and 9(b) show the streamlines for two nanofluids of water-Al_2O_3 and kerosene-Al_2O_3, respectively. These figures indicate that the presence of nanoparticles could affect the patterns of the streamlines. The most affected regions are near the center of the cavity.

Figure 10 shows the effect of the size of nanoparticles, Group No. 2, as a function of Rayleigh number. Comparison between 21 nm AL_2O_3 nanoparticles and 44 nm AL_2O_3 nanoparticles in kerosene indicates that the small nanoparticles (21 nm) show higher

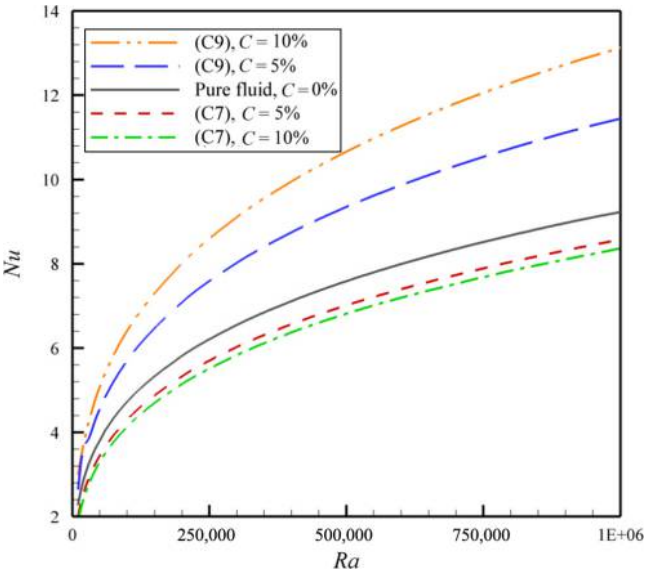

Figure 7.
Comparison of average Nusselt number between base-fluids of water-AL_2O_3 (C7) and Kerosene-AL_2O_3 (C9) nanofluids

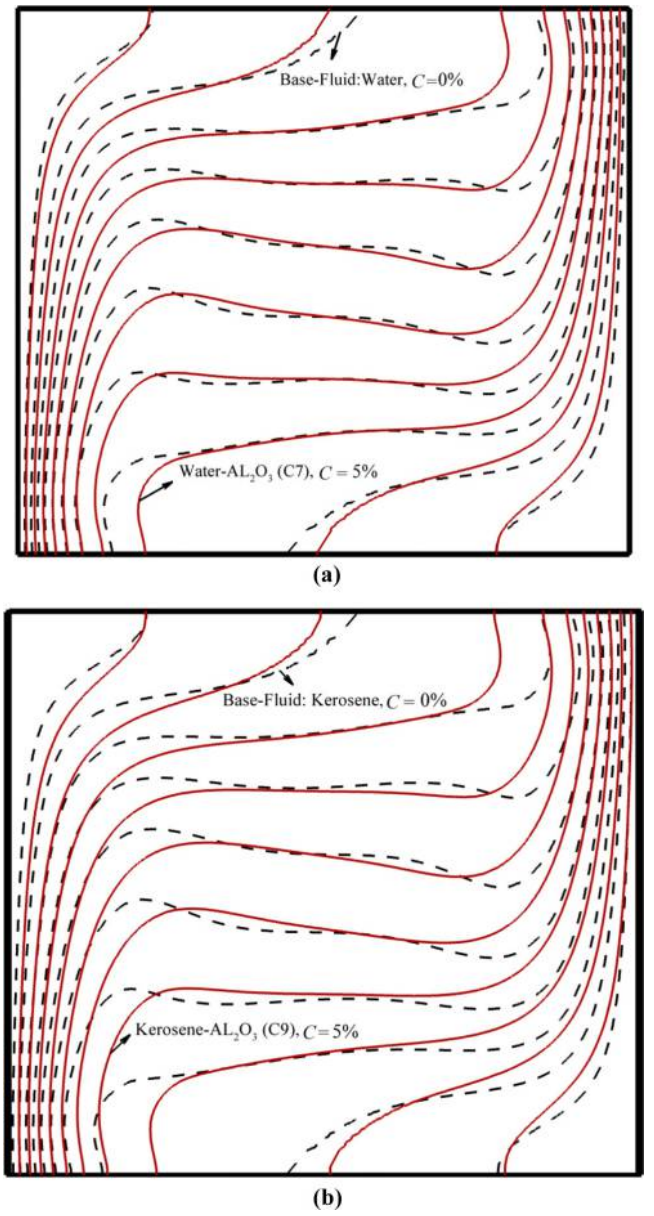

Figure 8.
Comparison between isothermal contours of base-fluids and nanofluids for (a) water and water-AL_2O_3 (b) kerosene and kerosene-AL_2O_3, in $Ra = 10^5$ and $C = 5$ per cent

average Nusselt number than those of 44 nm. Table V shows that the thermal conductivity parameter (*Nc*) and the dynamic viscosity parameters (*Nv*) of the samples containing 21 nm alumina nanoparticles are higher than those of 44 nm. As observed in the non-dimensional analysis, the increase of the thermal conductivity parameter tends to enhance the convective

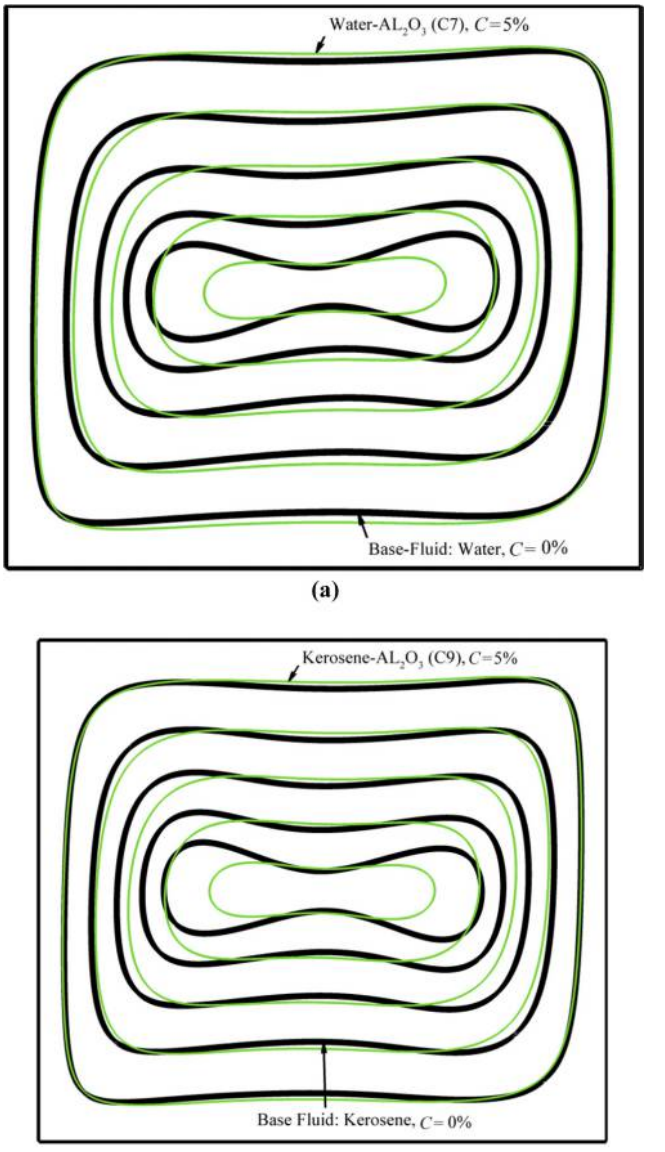

Figure 9.
A comparison between streamlines of base fluid and nanofluid

Notes: (a) Water and water-AL_2O_3 (b) kerosene and kerosene-AL_2O_3 in $Ra = 105$ and $C = 5$ per cent

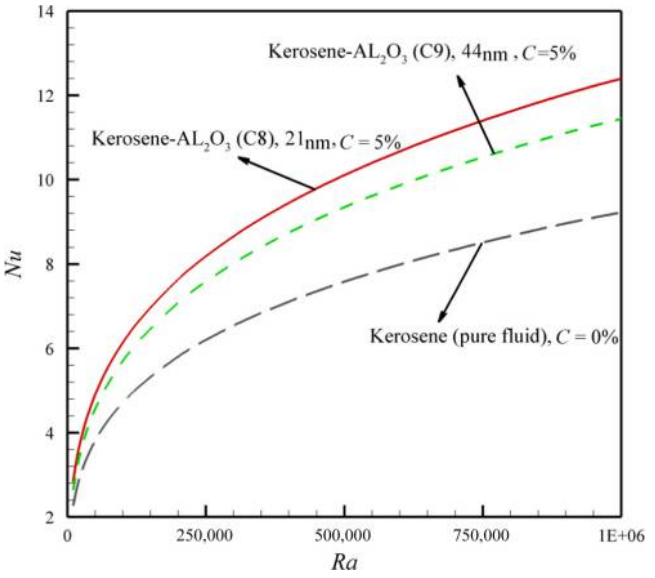

Figure 10.
The effect of size of nanoparticles on the average Nusselt number for Group No. 2

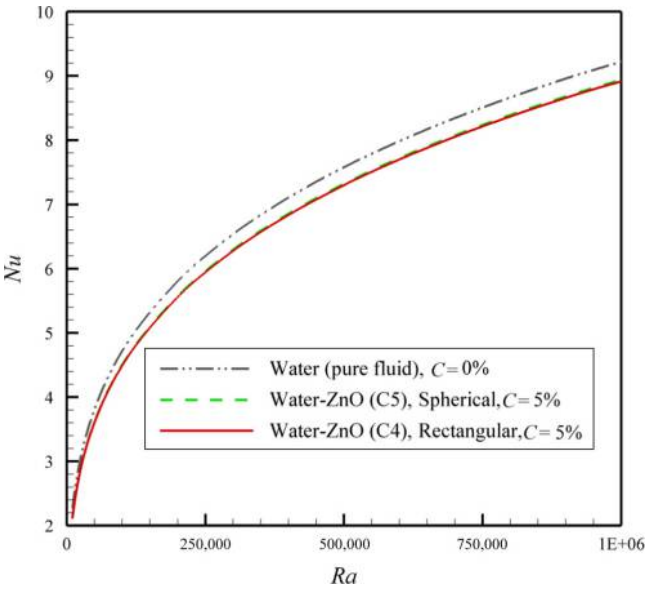

Figure 11.
Effect of shape of nanoparticles on the natural convective heat transfer

heat transfer; in contrast, the increase of the dynamic viscosity parameter tends to reduce the heat transfer. The non-dimensional analysis was also revealed that both of the dynamic viscosity and thermal conductive parameters are important for small Rayleigh numbers, but, when the Rayleigh number is large, the thermal conductivity parameter is the dominant effect. Hence, this figure in agreement with the non-dimensional analysis reveals that the

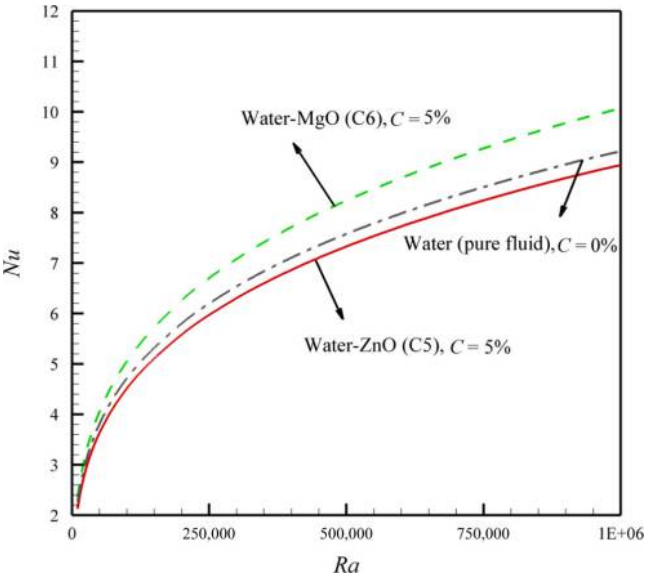

Figure 12.
Effect of type of nanoparticles on the convective heat transfer

both curves of C8 and C9 are almost coincident for small values of Rayleigh number, but, for large values of Rayleigh number, the difference between these curves is magnified, and the curves become completely distinct. This is because of the fact that the decrease of the size of nanoparticles increases both of the thermal conductivity and dynamic viscosity parameters. For small Rayleigh numbers, both of these effects, i.e. *Nc* and *Nv*, are important, and, hence, the curves are close together. As the Rayleigh number increases the dominant effect is the thermal conductivity parameter, and, hence, the average Nusselt number for smaller nanoparticles (21 nm) is higher than that of the larger nanoparticles (44 nm). The gray line in Figure 10 shows the average Nusselt number of the base fluid (i.e. $C = 0$ per cent). As seen, the presence of nanoparticles results in enhancement of the convective heat transfer for both of the 21 and 44 nm nanoparticles in kerosene. In the boundary-layer analysis of the heat transfer of nanofluids, the enhancement of 21 nm alumina nanoparticles was higher than that of 44 nm. However, the observed enhancement in the Nusselt number was independent of the Rayleigh number (Zaraki *et al.*, 2015).

Figure 11 depicts the effect of the shape of nanoparticles on the average Nusselt number. This figure compares the evaluated average Nusselt number for the nanofluid of Group No. 3. According to this figure, nanoparticles with spherical shape show higher average Nusselt number than nanoparticles with rectangular shape. Considering the values of *Nc* and *Nv* in Table V and attention to the separation curves in Figure 5 show that the sets of *Nc* and *Nv* for both of the under investigation nanofluids are placed above the separation lines, and, hence, the presence of nanoparticles in the base fluid deteriorates the convective heat transfer rate. The comparison between the gray curve, corresponding to the average Nusselt number of the base fluid, and the curves of C4, and C5 also confirms the reduction of the average Nusselt number by the presence of nanoparticles. The curves of C4 and C5 are very close together; this is because of the fact that the *Nc* and *Nv* for these two nanofluids are very close. It is also clear that utilizing rectangular shape nanoparticles results in higher deterioration of heat transfer rather than the spherical ones, but the differences are smooth.

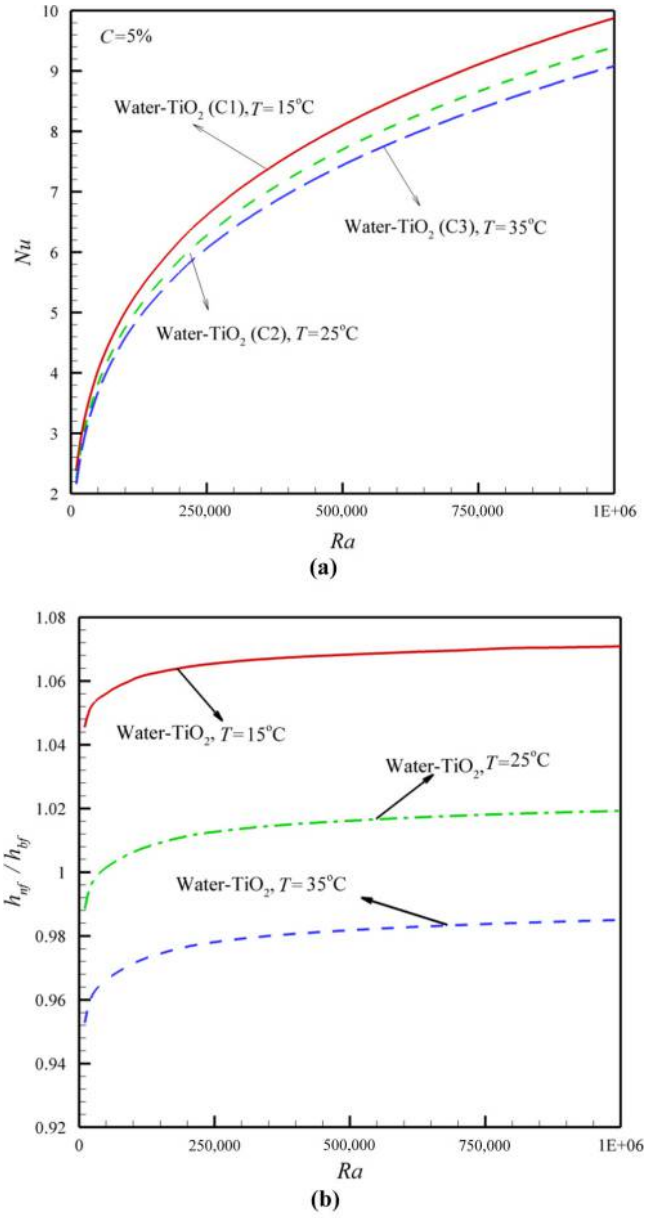

Notes: (a) Average Nusselt number; (b) the enhancement ratio

Figure 13.
The effect of working temperature on the enhancement ratio (h_{nf}/h_{bf}) as a function of the Rayleigh number when $C = 5$ per cent

In contrast with the results of the present study, the boundary analysis for the heat transfer of nanofluids indicates that the presence of ZnO nanoparticles in the base fluid results in the enhancement of heat transfer (Zaraki *et al.*, 2015).

Figure 12 illustrates the effect of the type of nanoparticles on the convective heat transfer. The results are plotted for the nanofluids of Group No. 4. The base fluid for both nanofluids is water at 25°C, and the size and shape of nanoparticles for both nanofluids are identical. The difference between the nanofluids is the constitutive martial of the nanoparticles. The nanofluid C5 is synthesized by ZnO nanoparticles, whereas C6 is synthesized by MgO nanoparticles. The gray line shows the average Nusselt number for the base fluid. As seen, utilizing the MgO nanoparticles results in significant enhancement of the natural convective heat transfer, but utilizing ZnO nanoparticles results in significant deterioration of the convective heat transfer in the enclosure. This figure indicates that the type of nanoparticles is very important. Utilizing the proper type of nanoparticles could results in significant enhancement in the convective heat transfer, but insufficient nanoparticles could significantly deteriorate the convective heat transfer.

Figure 13(a) and 13(b) shows the effect of working temperature on the average Nusselt number and the enhancement ratio for the nanofluids in Group No. 5. As seen, the raise of the working temperature reduces the convective heat transfer. Figure 13 (b) shows that the effect of the working temperature on the convective heat transfer of nanofluids is very important. For example, utilizing TiO_2-water nanofluid in low temperatures, 15°C, always enhances the convective heat transfer. In contrast, utilizing the same nanofluid, i.e. TiO_2-water, in comparatively high temperatures, 35°C, always deteriorates the convective heat transfer. Using the TiO_2-water nanofluid with the temperature about 25°C results in enhancement of convective heat transfer for comparatively high values of the Rayleigh number but using the same nanofluid results in deterioration of the natural convective heat transfer for very low values of the Rayleigh number. This is a very crucial point for utilizing nanofluids in natural convective systems. When a system goes to a failure or an over heat situation, in which the temperature of the system raises, the efficiency of the natural convective heat transfer of the nanofluid reduces or in some cases the enhancement may be changes to deterioration of the convective heat transfer. This issue could significantly limit the boundary of utilizing nanofluids for decreasing the size of the heat transfer systems. The same trend of results was also reported in the study of Zaraki *et al.* (2015) for the boundary layer heat transfer of nanofluids.

6. Conclusion

The natural convection heat transfer of nanofluids in a square cavity is theoretically analyzed. The governing equations, invoking the definition of thermal conductivity (*Nc*) and dynamic viscosity parameters (*Nv*), were transformed into a non-dimensional form and solved using the finite element method. The outcomes reveal that the most significant parameters on the analysis of the convective heat transfer of nanofluids in the enclosure are the thermal conductivity parameter (*Nc*), the dynamic viscosity parameter (*Nv*) and the Rayleigh number (*Ra*). The effect of other non-dimensional parameters such as the density ratio (ρ_{nf}/ρ_{bf}), the buoyancy ratio $(\rho\beta)_{nf}/(\rho_{nf}\beta_{bf})$ and the Prandtl number on the convective heat transfer of nanofluids was found negligible. As known, the presence of nanoparticles in the base fluid would enhance both of the thermal conductivity and dynamic viscosity parameters. The results of the present study reveal that the increase of the thermal conductivity parameter tends to enhance the heat transfer, but the increase of the dynamic viscosity parameter tends to decrease the convective heat transfer. Hence, based on the magnitude of the enhancement in the thermal conductivity and the dynamic viscosity,

induced by the presence of nanoparticles, the natural convective heat transfer in the enclosure can be enhanced or deteriorated. In the present study and by utilizing a non-dimensional analysis, the separation lines were found and reported as a function of thermal conductivity parameter (*Nc*) and dynamic viscosity parameter (*Nv*) for various values of the Rayleigh number. The separation lines indicate the boundaries, $h_{nf}/h_{bf} = 1$, in which using nanofluids starts to enhance the convective heat transfer.

Furthermore, the effect of the size of nanoparticles, type of nanoparticles, the shape of nanoparticles, the type of the base fluids and the working temperature were also examined through some case studies. The main outcomes can be summarized as follows:

- The increase of the Rayleigh number increases the enhancement of using nanofluids. When the Rayleigh number increases, the presence of the nanoparticles in the nanofluid tends to boost the convective heat transfer and results in further enhancement in the convective heat transfer and heat removal from the hot wall.
- The variation of Rayleigh number alters the position of the separation lines. Hence, the presence of nanoparticles for a nanofluid may enhance the convective heat transfer for high values of the Rayleigh numbers. However, the deterioration of the convective heat transfer may be seen for the nanofluid at the low values of the Rayleigh numbers.
- The effect of the shape of nanoparticles on the enhancement of the convective heat transfer is almost negligible. The increase of the size of nanoparticles increases the convective heat transfer.
- The type of nanoparticles and the base fluid significantly affect the enhancement of nanofluids. Using adequate nanoparticles in a base fluid could result in significant enhancement in the convective heat transfer of nanofluids. The inadequate choose of nanoparticles could also result in significant deterioration of the natural convective heat transfer.
- The working temperature affects the enhancement of using nanofluids. The increase of the working temperature decreases the efficiency of the nanofluid. This is an important issue in application of nanofluids and could limit the capability of nanofluids in reducing the size of the heat removal systems.

References

Abu-Nada, E. (2009), "Effect of variable viscosity and thermal conductivity of AL_2O_3-water nanofluid on heat transfer enhancement in natural convection", *International Journal of Heat and Fluid Flow*, Vol. 30 No. 4, pp. 679-690.

Agarwal, D.K., Vaidyanathan, A. and Sunil Kumar, S. (2013), "Synthesis and characterization of kerosene-Alumina nanofluids", *Applied Thermal Engineering*, Vol. 60 No. 1, pp. 275-284.

Baïri, A., Garcia de Maria, J.M., Alilat, N., Laraqi, N. and Bauzin, J.G. (2015), "Nu-Ra correlations for natural convection at high Ra numbers in air-filled tilted hemispherical cavities with dome oriented upwards: disk submitted to constant heat flux", *International Journal of Numerical Methods for Heat and Fluid Flow*, Vol. 25 No. 3, pp. 504-512.

Baïri, A., Zarco-Pernia, E. and García de María, J.M. (2014), "A review on natural convection in enclosures for engineering applications the particular case of the parallelogrammic diode cavity", *Applied Thermal Engineering*, Vol. 63 No. 1, pp. 304-322.

Basak, T., Roy, S. and Balakrishnan, A.R. (2006a), "Effects of thermal boundary conditions on natural convection flows within a square cavity", *International Journal of Heat and Mass Transfer*, Vol. 49 No. 23, pp. 4525-4535.

Basak, T., Roy, S., Paul, T. and Pop, I. (2006b), "Natural convection in a square cavity filled with a porous medium: effects of various thermal boundary conditions", *International Journal of Heat and Mass Transfer*, Vol. 49 No. 7, pp. 1430-1441.

Brinkman, H.C. (1952), "The viscosity of concentrated suspensions and solutions", *Journal of Chemical Physics*, Vol. 20 No. 4, pp. 571-571.

Buongiorno, J., Venerus, D.C., Prabhat, N., McKrell, T., Townsend, J. and Christianson, R. (2009), "A benchmark study on the thermal conductivity of nanofluids", *Journal of Applied Physics*, Vol. 106 No. 9, pp. 094312.

Ceramaret, S.D.B. (2013), *Physical, Mechanical, Thermal, Electrical and Chemical Properties*, Bôle, available at: http://archive.is/0Brd9

Chandrasekar, M., Suresh, S. and Chandra Bose, A. (2010), "Experimental investigations and theoretical determination of thermal conductivity and viscosity of Al2O3/water nanofluid", *Experimental Thermal and Fluid Science*, Vol. 34 No. 2, pp. 210-216.

Duangthongsuk, W. and Wongwises, S. (2009), "Measurement of temperature-dependent thermal conductivity and viscosity of TiO2-water nanofluids", *Experimental Thermal and Fluid Science*, Vol. 33 pp. 706-714.

Einstein, A. (1956), *Investigation on the Theory of Brownian Motion*, Dover, New York, NY.

Esfe, H.M., Saedodin, S. and Mahmoodi, M. (2014), "Experimental studies on the convective heat transfer performance and thermophysical properties of MgO–water nanofluid under turbulent flow", *Experimental Thermal and Fluid Science*, Vol. 52 pp. 68-78.

Ghadimi, A. and Metselaar, I.H. (2013), "The influence of surfactant and ultrasonic processing on improvement of stability, thermal conductivity and viscosity of titania nanofluid", *Experimental Thermal and Fluid Science*, Vol. 51 pp. 1-9.

Ghadimi, A., Saidur, R. and Metselaar, H.S.C. (2011), "A review of nanofluid stability properties and characterization in stationary conditions", *International Journal of Heat and Mass Transfer*, Vol. 54 No. 17, pp. 4051-4068.

Hussain, S. and Hussein, A. (2014), "Natural convection heat transfer enhancement in differentially heated enclosure filled with copper-water nanofluid", *Journal of Heat Transfer*, Vol. 136 No. 8, p. 082502.

Hwang, K.S., Lee, J.H. and Jang, J.P. (2007), "Buoyancy-driven heat transfer of water-based Al_2O_3 nanofluids in a rectangular cavity", *International Journal of Heat and Mass Transfer*, Vol. 50 No. 19, pp. 4003-4010.

Ismael, M.A., Pop, I. and Chamkha, A.J. (2014), "Mixed convection in a lid driven square cavity with partial slip", *International Journal of Thermal Sciences*, Vol. 82 pp. 47-61.

Jang, S.P. and Choi, S.U.S. (2004), "The role of Brownian motion the enhanced thermal conductivity of nanofluids", *Applied Physics Letters*, Vol. 84 No. 21, pp. 4316-4318.

Jeong, J., Li, C., Kwon, Y., Lee, J., Kim, S.H. and Yun, R. (2013), "Particle shape effect on the viscosity and thermal conductivity of ZnO nanofluids", *International Journal of Refrigeration*, Vol. 36 No. 8, pp. 2233-2241.

Kahveci, K. (2010), "Buoyancy driven heat transfer of nanofluids in tilted enclosure", *Journal of Heat Transfer*, Vol. 132 No. 6, p. 062501.

Kakaç, S. and Pramuanjaroenkij, A. (2009), "Review of convective heat transfer enhancement with nanofluids", *International Journal of Heat and Mass Transfer*, Vol. 52 No. 13, pp. 3187-3196.

Khanafer, K. and Vafai, K. (2011), "A critical synthesis of thermophysical characteristics of nanofluids", *International Journal of Heat and Mass Transfer*, Vol. 54 No. 19, pp. 4410-4428.

Lee, G.J., Kim, Ch, K., Lee, M.K., Rhee, C.K., Kim, S. and Kim, C. (2012), "Thermal conductivity enhancement of ZnO nanofluid using a one-step physiccal method", *Thermo Chimica Acta*, Vol. 542 pp. 24-27.

Lin, K.C. and Violi, A. (2010), "Natural convection heat transfer of nanofluids in a vertical cavity, effects of non-uniform particle diameter and temperature on thermal conductivity", *International Journal of Heat and Fluid Flow*, Vol. 31 No. 2, pp. 236-245.

Lotfizadeh Dehkordi, B., Ghadimi, A. and Metselaar, H.S.C. (2013), "Box–Behnken experimental design for investigation of stability and thermal conductivity of TiO2 nanofluids", *Journal of Nanoparticle Research*, Vol. 15 No. 1, pp. 1-9.

Makinde, D. (2013), "Effects of viscous dissipation and Newtonian heating on boundary-layer flow of nanofluids over a flat plate", *International Journal of Numerical Methods for Heat and Fluid Flow*, Vol. 23 No. 8, pp. 1291-1303.

Mansour, M.A., Bakeir, M.A. and Chamkha, A. (2014), "Natural convection inside a C-shaped nanofluid-filled enclosure with localized heat sources", *International Journal of Numerical Methods for Heat and Fluid Flow*, Vol. 24 No. 8, pp. 1954-1978.

Maxwell, J.C. (1881), *A treatise on Electricity and Magnetism*, Clarendon, Oxford.

Nasrin, R., Alim, M.A. and Chamkha, A.J. (2013), "Numerical simulation of non-darcy forced convection through a channel with non-uniform heat flux in an open cavity using nanofluid", *Numerical Heat Transfer*, Vol. 64 No. 10, pp. 820-840.

Noghrehabadi, A., Samimi Behbahan, A. and Pop, I. (2015), "Thermophoresis and brownian effects on natural convection of nanofluids in a square enclosure with two pairs of heat source/sink", *International Journal of Numerical Methods for Heat and Fluid Flow*, Vol. 25 No. 5, pp. 1030-1046.

Pak, B.C. and Cho, Y. (1998), "Hydrodynamic and heat transfer study of dispersed fluids with submicron metallic oxide particle", *Experimental Heat Transfer an International Journal*, Vol. 11 No. 2, pp. 151-170.

Parvin, S. and Chamkha, A.J. (2014), "An analysis on free convection flow, heat transfer and entropy generation in an odd-shaped cavity filled with nanofluid", *International Communications in Heat and Mass Transfer*, Vol. 54 pp. 8-17.

Patrulescu, F.O., Grosan, T. and Pop, I. (2014), "Mixed convection boundary layer flow from a vertical truncated cone in a nanofluid", *International Journal of Numerical Methods for Heat and Fluid Flow*, Vol. 24 No. 5, pp. 1175-1190.

Reddy, J.N. (1993), *An Introduction to the Finite Element Method*, McGraw-Hill, New York, NY.

Sadollah, A., Ghadimi, A., Metselaar, I.H. and Bahreininejad, A. (2013), "Prediction and optimization of stability parameters for titanium dioxide nanofluid using response surface methodology and artificial neural networks", *Science and Engineering of Composite Material*, Vol. 20 No. 4, pp. 319-330.

Sarkar, J. (2011), "A critical review on convective heat transfer correlations of nanofluids", *Renewable and Sustainable Energy Reviews*, Vol. 15 No. 6, pp. 3271-3277.

Sathiyamoorthy, M. and Chamkha, A.J. (2014), "Analysis of natural convection in a square cavity with a thin partition for linearly heated side walls", *International Journal of Numerical Methods for Heat and Fluid Flow*, Vol. 24 No. 5, pp. 1057-1072.

Sheikholeslami, M., E., R., Hassan, M. and Soliemani, S. (2014), "A study of natural convection heat transfer in a nanofluid filled with elliptical inner cylinder", *International Journal of Numerical Methods for Heat and Fluid Flow*, Vol. 24 No. 8, pp. 1906-1927.

Sundar, L.S., Sharma, K.V., Naik, M.T. and Singh, M.K. (2013), "Empirical and theoretical correlations on viscosity of nanofluids: a review", *Renewable and Sustainable Energy Reviews*, Vol. 25 pp. 670-686.

ToolBox, E. (2013a), "Constant pressure heat capacity of water vs temperature", available at: www.engineeringtoolbox.com/water-thermal-properties-d_162.html (accessed 11 January 2013).

ToolBox, E. (2013b), "Fuels, densities and specific volumes propertices", available at: www.engineeringtoolbox.com/fuels-densities-specific-volumes-d_166.html (accessed 11 January 2013).

Turan, O., Sachdeva, A., Chakraborty, N. and Poole, J.R. (2011), "Laminar natural convection of power-law fluids in a square enclosure with differentially heated side walls subjected to constant temperatures", *Journal of Non-Newtonian Fluid Mechanics*, Vol. 166 No. 17, pp. 1049-1063.

Venerus, D.C., Buongiorno, J., Christianson, R., Townsend, J., Bang, I.C. and Chen, G. (2010), "Viscosity measurements on colloidal dispersions (nanofluids) for heat transfer applications", *Applied Rheology*, Vol. 20 No. 4.

Zaraki, A., Ghalambaz, M., Chamkha, A.J., Ghalambaz, M. and De Rossi, D. (2015), "Theoretical analysis of natural convection boundary layer heat and mass transfer of nanofluids: effects of size, shape and type of nanoparticles, type of base fluid and working temperature", *Advanced Powder Technology*, Vol. 26 No. 3, pp. 935-946.

Corresponding author
Ali Chamkha can be contacted at: achamkha@yahoo.com